Journal of Luminescence 131 (2011) 502–505

Contents lists available at ScienceDirect

Journal of Luminescence

journal homepage: www.elsevier.com/locate/jlumin

Plasmon resonance modulated photoluminescence and Raman spectroscopy of diindenoperylene organic semiconductor thin film

D. Zhang [a,*], A. Horneber [a], J. Mihaljevic [a], U. Heinemeyer [b], K. Braun [a], F. Schreiber [b], R. Scholz [c], A.J. Meixner [a,*]

[a] Institut für Physikalische und Theoretische Chemie, University of Tübingen, 72076 Tübingen, Germany
[b] Institut für Angewandte Physik, University of Tübingen, 72076 Tübingen, Germany
[c] Institut für Angewandte Photophysik, Technische Universität Dresden, 01062 Dresden, Germany

ARTICLE INFO

Available online 15 September 2010

Keywords:
Organic semiconductor thin film
Photoluminescence
Plasmon resonator

ABSTRACT

In a comparison between a bare diindenoperylene (DIP) film and a DIP film spin-coated with a layer of gold nanoparticles, we have investigated the influence of plasmon resonances in the gold particles on spectroscopic properties of the molecular film. Under off-resonant excitation with a laser at 633 nm, the bare DIP film showed only weak photoluminescence (PL) and Raman signals, but after spin-coating gold nanoparticles on such a DIP film, we found an enhancement of both the PL and Raman signals by a factor of about 3, whereas no enhancement could be observed when the same sample was excited with laser light of 488 nm. This difference reveals that at 633 nm, plasmon resonances in the gold nanoparticles are excited, leading in turn to an enhancement of PL and Raman signals of the weakly absorbing DIP film via coupling between plasmons in the gold particles and exciton–polaritons in the molecular film. For the laser at 488 nm, due to a much larger absorption coefficient of DIP, excitons in the molecular film are directly excited, out-weighing the influence of an off-resonant coupling to the plasmon resonances in the gold particles occurring at much lower energy.

1. Introduction

During the last decades, semiconducting organic materials have been studied intensively due to their interesting opto-electronic properties, giving rise to a broad range of applications [1] such as organic field effect transistors, organic light emitting diodes or organic solar cells. Diindenoperylene (DIP) is one of the promising semiconducting organic materials since it forms closed films with high structural order, relatively large hole mobility and rather long exciton diffusion length [2]. The optical response of dissolved DIP molecules is dominated by the π–π^* HOMO–LUMO transition, revealing a strong coupling of the optical excitation to internal vibrations around 0.17 eV. In the crystalline phase, this spectroscopic fingerprint of the excited monomer is modified by the interference between charge transfer states involving stack neighbours and Frenkel excitons consisting of Bloch waves formed from neutral molecular excitations [3–6].

Surface plasmon resonances in metallic nanoparticles can produce a large enhancement of local electric field in their immediate surroundings. This phenomenon can be exploited for an increased optical absorption resulting in a larger photocurrent in p–n junctions [7] and for surface enhanced Raman scattering, allowing detection of single molecules [8,9]. The field enhancement is restricted to a small volume around each nanoparticle, so that the combination of plasmonic resonances with scanning probe techniques can simultaneously achieve a strongly enhanced optical response together with a high spatial resolution [10]. As demonstrated recently, placing a sharp gold tip as a local probe within a few nanometers from the sample surface into the focus of a parabolic mirror, the strong plasmonic enhancement of the local electric field around the tip apex can be used for a highly localized excitation of a sample of interest, in our case, a DIP film [11]. Moreover, the evanescent electric field around the tip alters the photonic density of states, modifying in turn the spontaneous emission rate from the excitons in the molecular material directly underneath [10,12]. Based on this excitation and detection scheme, dramatically enhanced photoluminescence (PL) and Raman spectra from DIP could be observed together with spatially resolved monomolecular steps of highly ordered DIP films, which revealed a localized 'shining-edge effect', with a further enhancement of PL by a factor of about 4 with respect to flat surface regions [11].

In the present work, we investigate the influence of gold nanoparticles on Raman scattering and PL emission from a semiconducting DIP thin film for two laser lines either resonant (633 nm) or off-resonant (488 nm) with respect to plasmon modes in the metallic nanoparticles, revealing how the Raman

* Corresponding authors.
E-mail addresses: dai.zhang@uni-tuebingen.de (D. Zhang), alfred.meixner@uni-tuebingen.de (A.J. Meixner).

0022-2313/$ - see front matter © 2010 Elsevier B.V. All rights reserved.
doi:10.1016/j.jlumin.2010.09.008

and PL processes are influenced by the respective resonance conditions. Finite-difference time-domain (FDTD) simulations of the interaction between the enhanced electric field around the spherical gold particles and the DIP films are used for an interpretation of the experimental findings.

2. Material and methods

All samples were prepared on smooth Si(1 0 0) substrates covered by 150 nm of SiO_2. DIP layers of 20 nm thickness were grown at a substrate temperature of 130 °C at a rate of 12 ± 3 Å/min under UHV conditions, leading to films of high structural order. 20 μL gold nanoparticles (20 nm diameter) were deposited on these films (Sigma-Aldrich, 1:20 diluted in water) by dropping the aqueous suspension onto the DIP thin film surface. The sample was then rotated at a speed of 3200 rpm to spin-coat the gold nanoparticles over the surface. Optical properties of the DIP sample are measured on a home-built confocal optical microscope [13,14]. Instead of an objective lens, this microscope uses a parabolic mirror (numerical aperture 0.998) for laser focusing and signal collection. This instrument yields a small focal spot with an area of $0.134\lambda^2$. The excitation laser beam is directed to this parabolic mirror and reflected onto the sample surface coinciding with the focal plane of the mirror. Either radial or azimuthally polarized laser beams were used for the measurements. For azimuthal polarization, the electric field distributes exclusively in the *xy* focal plane. For radial polarization of the laser beam in the focal region the electric field is mainly polarized along the sample normal *z* (93.5% intensity at 633 nm) with a marginal intensity (6.5%) polarized within the *xy* focal plane [15]. The optical signal is detected either by a CCD coupled spectrometer (600 grating) or by an avalanche photodiode detector (APD) for PL imaging.

3. Results and discussion

3.1. Excitation of DIP thin film with 488 nm (2.54 eV) laser

The HOMO–LUMO transition of crystalline DIP has a maximum at 2.25 eV (551 nm) corresponding to the first absorption peak (0-0) of the optical response. The spacing of the vibronic progression still resembles the one for dissolved monomers, but the relative strength of different subbands can be understood only from an in-depth analysis of the interference between Frenkel excitons and CT transitions [3–6].

Fig. 1a shows the resonant Raman spectra collected from a 20 nm thick DIP film under excitation at 488 nm polarized either radially (spectrum I) or azimuthally (spectrum II). With radially polarized excitation, clear Raman features (inset of Fig. 1a) appeared at 520, 634, 1284, 1395, 1459 and 1608 cm^{-1}. Except for the intense Raman peak at 520 cm^{-1} and a broad 2 phonon band around 960 cm^{-1} originating from the Si substrate [16], all other Raman cross-sections can be assigned to the in-plane C–C stretching vibrations and C–H bending modes of a DIP molecule [4,17]. The PL from DIP increases towards larger Stokes shift, saturating the detector above 2750 cm^{-1}. Non-saturated PL spectra covering the range between 1.75 and 2.40 eV are shown in Fig. 1b. A small mismatch between four adjacent detection windows results from the energy-dependent detection efficiency of the camera. The intensity maxima located at 1.81, 1.97 and 2.14 eV correspond to similar PL features reported earlier [18].

When switching the polarization to the azimuthal mode, where the electric field is restricted to the *xy* focal plane, a much smaller Raman spectrum (inset of Fig. 1a) was collected. The Si Raman peak at 520 cm^{-1} in spectrum II amounts to only 56% of its intensity in spectrum I due to its polarization-dependent Raman cross-section at this excitation wavelength. The Raman intensities assigned to DIP decreased more strongly, for the Raman peak at 1284 cm^{-1} to about 20% of the intensity with radially polarized excitation. This reduction is somewhat larger than that of the ratio of the respective PL intensities, amounting to about 30%. Previous investigations of similar DIP films have demonstrated that the transition dipole oriented along the long axis of the molecules is tilted by about $\theta \approx 17°$ against the substrate normal, so that a more efficient interaction with light polarized along the substrate normal can be expected, as realized for radial polarization of the laser beam [3,11].

3.2. Plasmonic enhancement for excitation with 633 nm (1.96 eV) laser

In this section, we compare the spectra obtained from a bare DIP film and from a DIP film after deposition of gold nanoparticles. In the latter case, the laser at 633 nm (1.96 eV) is expected to result in an efficient coupling to the plasmonic resonances in the gold spheres, yielding eventually a moderate enhancement of the spectroscopic response of DIP.

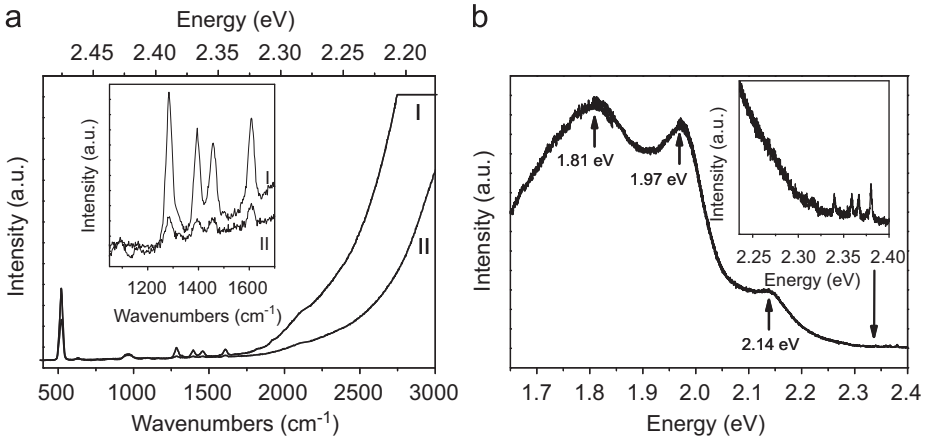

Fig. 1. (a) Spectra collected with a confocal parabolic-mirror microscope from DIP thin film with 488 nm excitation, integration time 60 s. I: with polarization perpendicular to the sample surface (radially polarized laser) and II: with polarization in the sample plane (azimuthally polarized laser). Inset : spectra I and II on an enlarged scale highlighting the Raman features. (b) PL spectra collected over four adjacent spectral detection windows for polarization perpendicular to the sample surface (radially polarized laser beam), integrated over 10 s for each spectrum. Inset: enlarged spectrum of the region with the strongest Raman features of DIP.

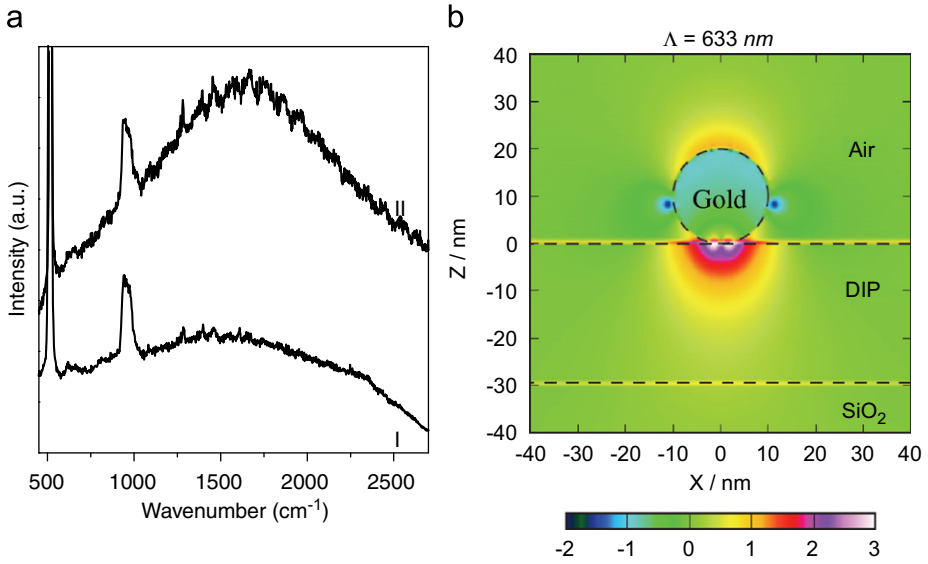

Fig. 2. (a) Spectra collected for excitation at 633 nm with radial polarization. I: DIP film, spectrum integrated over 60 s and II: DIP film covered with gold nanoparticles, spectrum integrated over 60 s. Laser power: 170 μW. (b) Field intensity for excitation of a gold nanosphere with a diameter of 20 nm on top of a DIP film with a thickness of 30 nm, for polarization along the sample normal *z*. The results of a FDTD simulation are reported on a logarithmic scale corresponding to relative intensities of 10^{-2}–10^{3} with respect to the far field region.

Fig. 2a shows the spectra recorded from the DIP film with 633 nm illumination. The dominant Raman line at 520 cm^{-1} and the broad band around 960 cm^{-1} both arise from the Si substrate [16]. Raman and PL signals from the bare DIP film (spectrum I) were very weak. The positions of all the distinguishable Raman bands (1284, 1395, 1459 and 1608 cm^{-1}) are in good agreement with those observed when excited at 488 nm. The very weak PL and Raman intensities observed with an excitation laser of 633 nm are due to the inefficiency of the off-resonant excitation at 1.96 eV with respect to the 0–0 subband of crystalline DIP at 2.25 eV. Spectrum II was collected from the DIP thin film after deposition of Au nanoparticles. Despite the progressive oscillatory features being superimposed on the spectrum, the DIP Raman features remain clearly visible, and the PL background was significantly increased. The Si Raman features arise from the substrate region far away from the gold nanoparticles, so that no plasmonic enhancement can be expected. Therefore, normalizing the spectra to the respective Raman intensities of Si, for DIP we derived a PL and Raman enhancement factor of about 3. Confocal PL imaging has revealed an aggregation of the gold nanoparticles into larger clusters, which have a broad distribution of red-shifted plasmon resonances [19], as compared to that of the individual gold particles in well dispersed aqueous solution [20]. Hence, such particle aggregates must also lead to an enhancement of Raman and PL spectra arising from the DIP film underneath. This agrees well with our previous work based on tip-enhanced spectroscopic measurements, which demonstrated that the coupling between the longitudinal plasmonic resonance in the gold tip and the exciton–polariton in the underlying DIP film enhances the PL emission via the modified photonic mode density close to the tip apex [11]. Due to similarities between the tip-induced plasmon near field and the plasmon resonances arising from aggregated gold nanoparticles, the enhanced PL intensity of the DIP thin film with spin-coated gold particles can be assigned to the same coupling mechanism. This idea is corroborated by FDTD simulations of light intensity around a gold nanoparticle on top of the DIP film as visualized in b. For excitation with a laser at 633 nm at the gold–DIP interface an enhancement of light intensity of about 10^{3} can be expected. Due to a small fraction of the DIP surface being covered by gold nanoparticles, the observable average enhancement factors for PL and Raman signals remain much smaller.

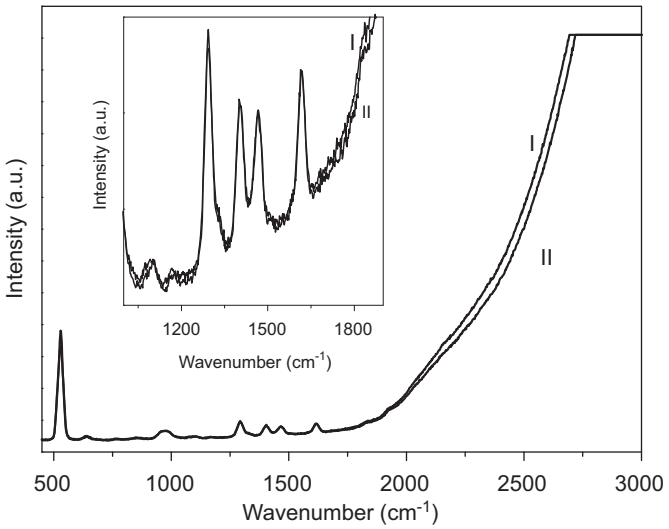

Fig. 3. Raman spectra integrated over 60 s for radially polarized laser beam at 488 nm. I: DIP film and II: DIP film covered with gold particles. Inset: enlarged spectrum covering the region with the largest Raman features of DIP.

For a comparison between the enhancement at 633 and 488 nm, DIP films with and without gold nanoparticles have been excited at 488 nm. The respective results in Fig. 3 demonstrate that spectrum I collected from a bare DIP film and spectrum II arising from a DIP film covered with gold nanoparticles exhibit similar Raman and PL intensities. In sharp contrast to excitation at 633 nm, at 488 nm no significant enhancement can be observed. This difference reveals that at 633 nm plasmon resonances in the gold nanoparticle aggregates lead to enhancement of absorption, PL and Raman scattering of the otherwise weakly absorbing DIP film via plasmon–exciton coupling. For 488 nm excitation, however, the situation is reversed. Due to the several orders of magnitude larger absorption cross-section of the DIP film in this

region, excitons in the molecular film can be created independently from the gold particles having their plasmon resonances at much lower energy. Hence, absorption, PL and Raman scattering from the DIP film are no more affected by the coupling between plasmons in the gold particles and exciton–polaritons in the organic material.

4. Conclusions

In summary, we have investigated Raman and PL spectra of 20 nm thick DIP films under resonant and off-resonant excitation conditions. Both the Raman and PL intensity are strongly polarization-dependent. With radially polarized excitation, the Raman signal is about 5 times stronger than azimuthally polarized excitation. On excitation at 633 nm, plasmon resonances of gold nanoparticles spin-coated onto the DIP thin film can be excited more efficiently than excitation at 488 nm, inducing a strong plasmon resonance in aggregates of nanoparticles. Accordingly, only at the longer excitation wavelength, the efficient coupling between the plasmon resonance in the gold nanoparticles and the exciton–polaritons in DIP enhances both the Raman and the PL spectra from the molecular semiconductor.

Acknowledgements

We thank Jens Pflaum for the purification of diindenoperylene used in the present work. Financial support from the Deutsche Forschungsgemeinschaft (ME1600/5-2, ME1600/12-1 and SCHR700/13-1), the 'Kompetenznetz Funktionelle Nanostrukturen' and Projektförderung für NachwuchswissenschaftlerInnen an der Universität Tübingen (5577) is gratefully acknowledged.

References

[1] F. Schreiber, Phys. Status Solidi A 201 (2004) 1037.
[2] A.K. Tripathi, J. Pflaum, Appl. Phys. Lett. 89 (2006) 082103.
[3] U. Heinemeyer, R. Scholz, L. Gisslén, M.I. Alonso, J.O. Ossó, M. Garriga, A. Hinderhofer, M. Kytka, S. Kowarik, A. Gerlach, F. Schreiber, Phys. Rev. B 78 (2008) 085210.
[4] L. Gisslén, R. Scholz, Phys. Rev. B 80 (2009) 115309.
[5] U. Heinemeyer, K. Broch, A. Hinderhofer, M. Kytka, R. Scholz, A. Gerlach, F. Schreiber, Phys. Rev. Lett. 104 (2010) 257401.
[6] S. Kowarik, A. Gerlach, S. Sellner, F. Schreiber, L. Cavalcanti, O. Konovalov, Phys. Rev. Lett. 96 (2006) 125504.
[7] D.M. Schaadt, B. Feng, E.T. Yu, Appl. Phys. Lett. 86 (2005) 063106.
[8] K.A. Willets, R.P. van Duyne, Annu. Rev. Phys. Chem. 58 (2007) 267.
[9] W.E. Doering, S.M. Nie, J. Phys. Chem. B 106 (2002) 311.
[10] P. Anger, P. Bharadwaj, L. Novotny, Phys. Rev. Lett. 96 (2006) 113002.
[11] D. Zhang, U. Heinemeyer, C. Stanciu, M. Sackrow, K. Braun, L.E. Hennemann, X. Wang, R. Scholz, F. Schreiber, A.J. Meixner, Phys. Rev. Lett. 104 (2010) 056601.
[12] C.K. Carniglia, L. Mandel, K.H. Drexhage, J. Opt. Soc. Am. 62 (1972) 479.
[13] C. Stanciu, M. Sackrow, A.J. Meixner, J. Microsc. 229 (2008) 247.
[14] D. Zhang, X. Wang, K. Braun, H.-J. Egelhaaf, M. Fleischer, L. Hennemann, H. Hintz, C. Stanciu, C.J. Brabec, D.P. Kern, A.J. Meixner, J. Raman Spectrosc. 40 (2009) 1371.
[15] M.A. Lieb, A.J. Meixner, Opt. Express 8 (2001) 458.
[16] P.A. Temple, C.E. Hathaway, Phys. Rev. B 7 (1973) 3685.
[17] R. Scholz, L. Gisslén, B.-E. Schuster, M.B. Casu, T. Chassé, U. Heinemeyer, F. Schreiber, J. Chem. Phys. 134 (2011) 014504.
[18] M. Heilig, M. Domhan, H. Port, J. Lumin. 110 (2004) 290.
[19] M. Steiner, Ch. Debus, A.V. Failla, A.J. Meixner, J. Phys. Chem. C 112 (2008) 3103.
[20] P.N. Njoki, I.I.S. Lim, D. Mott, H-Y. Park, B. Khan, S. Mishra, R. Sujakumar, J. Luo, C.-J. Zhong, J. Phys. Chem. C 111 (2007) 14664.